Role of Surface Chemistry in Adhesion between ZnO Nanowires and Carbon Fibers in Hybrid Composites

Gregory J. Ehlert,*,§ Ulises Galan,§,# and Henry A. Sodano§,‡

§Mechanical and Aerospace Engineering, University of Florida, P.O. Box 116250, Gainesville, Florida 32611-6250, United States
#School of Matter, Transport, and Energy, Arizona State University, Mail Stop 6106, Tempe, Arizona 85287-6106, United States
‡Materials Science and Engineering, University of Florida, P.O. Box 116400, Gainesville, Florida 32611-6400, United States

ABSTRACT: Low interface strength is a persistent problem in composite materials and cascades to limit a variety of bulk material properties such as lamina shear strength. Whiskerization has long been pursued as a method to reinforce the interphase and improve both the single fiber interface strength as well as the bulk properties. Recent developments have shown that ZnO nanowire whiskerization can effectively improve the properties of a bulk composite without requiring the high temperatures that previous deposition processes needed. Although the efficacy of a ZnO nanowire interphase has been established, the mechanism for adhesion of the interphase to the fiber has not been identified. Specifically, the addition of the ZnO nanowires to the surface of the fibers requires that the ZnO nanowires have strong chemical adhesion to the fiber surface. This work will create a variety of chemical environments on the surface of the fibers through new and common chemical functionalization procedures and quantify the surface chemistry through X-ray photoelectron spectroscopy. The effect of fiber surface chemistry on the adhesion of the ZnO is assessed through single fiber fragmentation testing. The interface strength is found to strongly correlate with the concentration of ketone groups on the surface of the fibers. Following the experimental observations, liftoff of a ZnO crystal from a graphene surface was simulated with a variety of surface functionalizations. The computational models confirm the preference for ketone groups in promoting adhesion between ZnO and graphite.

KEYWORDS: ZnO nanowires, fiber reinforced composite, functionalization, interface
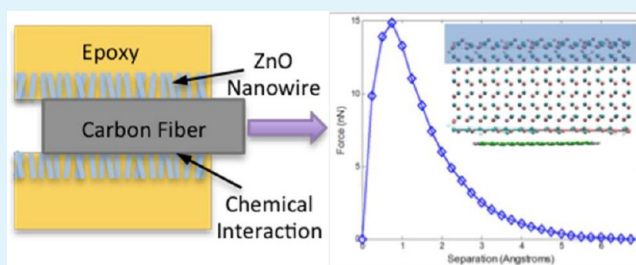
INTRODUCTION

Advanced fiber reinforced composite materials offer the high structural performance and low density demanded by the aerospace industry to meet mission requirements. Continuous fiber reinforced polymers (CFRPs) are the ideal material for aerospace structures, and they continue to be developed with significant research due to their high specific strength and stiffness. Unidirectional CFRPs offer superb performance in the fiber direction; however the performance is considerably lower when subjected to transverse or shear stresses. In CFRPs, the fiber is generally 1−3 orders of magnitude stiffer than polymer matrix, and loads transferred between fiber and matrix create high stress concentrations at the interface between the two.[1] Furthermore, the small diameter of typical reinforcing fibers leads to high surface area, thus increasing the portion of the material at the interface, which is affected by the stress concentration. Composite materials continue to be limited by the interface strength, and solutions with the ability to substantially improve various properties that heavily depend upon the interface do not currently exist.

The study of interfaces in composites was recognized as pivotal to the material's performance shortly after the advent of composite materials.[2] Researchers began to develop a variety of creative techniques to improve the interfacial strength, including chemical functionalization,[3−8] roughening,[9,10] and whiskerization.[2,11−20] Chemical functionalization focuses on the development of methods that modify the chemical state of the surface of the fiber to create functional groups that interact or crosslink with the polymer matrix. Chemical functionalization can be accomplished through a variety of plasma, grafting, or oxidative methods; however oxidative methods (chemical, electrochemical, plasma, thermal) tend to be the most used. Oxidative techniques are efficient, quick, inexpensive to set up, and effective for a variety of polymer matrices.[4,21−29] In spite of these advantages, oxidative techniques owe much of their effectiveness not to chemical interactions but rather to the roughening of the fiber accomplished during the oxidation reaction.[30] A rough interface interlocks with the surrounding polymer, increasing the surface area available for bonding across the interface. Zhdan et al. showed that this effect governs the performance of oxidative techniques and that many oxidative techniques are more accurately described as physical interface treatments.[30]

The current description of the interface in CFRPs is not an infinitely thin surface, but rather a solid volume of material designated the interphase.[31] Surfaces impose physical con-

straints on polymer motion and limit cross linking often causing the polymer near the interface surface to be significantly weaker and more compliant, thus producing an interphase with different properties than the bulk in most typical CFRPs. Modern manufacturers of structural fibers such as carbon and glass often coat the fibers in a polymeric sizing layer to correct problems associated with the natural formation of an interphase. The polymer coating on the fibers is designed to have appropriate mechanical properties in the presence of the surface and strongly interact with the polymer matrix to form a strong composite. Applying a polymer sizing layer to avoid the negative effects of the interphase is an effective method of interface enhancement, yet significant opportunities for improvement exist because the mechanical properties of polymers inherently create a stress concentration at the interface.

One promising alternative to interphase replacement is interphase reinforcement, specifically fiber whiskerization. Interphase reinforcement is most easily achieved through the growth of a secondary reinforcement on the surface of the structural fibers. Several materials are available for whiskerization, notably SiC whiskers,[2,16] carbon nanotubes (CNTs),[13-15] carbon nanofibers,[32] and more recently, ZnO nanowires.[17-19,33] Whiskerization is the process of growing a secondary fibrous material that protrudes radially from the structural fiber to strengthen the interphase and create a graded interface that reduces the stress concentration between the stiff fiber and compliant polymer. The deposition of SiC whiskers and carbon nanostructures on the surface of carbon fiber requires temperatures of 1300 °C[2] and 700 °C,[13-15,34] respectively, which reduces the tensile strength of the carbon fiber substrate due to reaction with the precursors and catalysts for growth. SiC whiskerization was originally claimed to enhance interface strength by as much as 300%,[2] and interfacial improvements in carbon nanotube whiskerized fibers as high as 71% have been reported.[14] Unlike CNTs and SiC whiskers, ZnO nanowires can be deposited on carbon fiber from aqueous solutions at temperatures below 90 °C,[35-37] enabling the deposition of whiskers with no impact to fiber tensile strength or fiber modulus. ZnO nanowire whiskerization has been shown to be very effective for improving the interface strength of carbon fiber composites, with single fiber interface strength enhancements of up to 228%[33] and has shown great ability to improve the bulk shear performance of a composite.[17] These levels of improvement are simply not achievable with polymer interphases or fiber sizing layers.

The presence of an interphase surrounding a fiber in a CFRP implies that instead of one interface, there are actually two. For a polymeric sizing layer or polymeric interphase, the strong interaction between the sizing layer and the polymer matrix generally leads to failure at the interphase/fiber interface, which benefits from the enhanced properties of the sizing layer. Sizing layers are typically optimized for adhesion of the sizing layer to the underlying structural fiber. Whisker interphases follow the same analysis; thus rather than a fiber/matrix interface, both the fiber/interphase and interphase/matrix interfaces must be superior to improve the effective composite properties. The whisker/matrix interface is much improved over the sizing/matrix interface because the whiskers interlock with the matrix, reinforce the interphase, and grade the interface to reduce the stress concentration that inevitably develops. The advantages of the ZnO whiskerization process stem primarily from the low temperature processing, which does not change the surface

roughness, surface area, or elastic properties of the fiber. The interlocking and gradient provided by the nanowires intuitively creates a strong interface; however the interaction between inorganic ZnO and organic carbon fibers is unexpected. The previous explanations of interface enhancement (roughness, stress concentration reduction, increased surface area, interlocking) do not congruently apply to the fiber/whisker interface; thus chemical adhesion is the next most likely explanation and is the subject of this work. Naturally, new methods of analysis and control must be developed to understand and improve the adhesion of whisker interphases to structural fibers.

This article will demonstrate the mechanism of adhesion between the fiber and whisker interphase in ZnO nanowire whiskerized composites. The focus is on the determination of what controls the whisker/fiber interface and assumes that the whisker/matrix interface is constant. The chemistry of adhesion will be the focus, rather than modulating the fiber roughness or surface area, because roughening can impact fiber tensile properties and eliminate a significant advantage of the ZnO whiskerization method. The surface of carbon fibers will be chemically modified while maintaining the surface roughness and surface area. Five specific chemical functionalization treatments will be created to modify the surface chemistry of carbon fibers. The five methods include one to reduce the surface of the fibers, two techniques to selectively create carboxylic acid groups and two techniques to produce a variety of oxygen functional groups. Each fiber will then be coated with ZnO nanowires and evaluated for interfacial shear strength using the single fiber fragmentation test. The contribution of a systematic experimental method for identifying and designing superior interphases represents a significant contribution to the scientific literature and could lead to higher strength composites, thus impacting the plethora of applications they find use in. Finally, the work concludes with a molecular dynamics (MD) model that simulates the liftoff of a ZnO crystal from a graphene surface. The computational model confirms the preference for ketone groups in promoting adhesion of the ZnO crystal to graphitic surfaces.

■ EXPERIMENTAL METHODS

Materials. IM-8 carbon fibers were received from Hexcel and washed in acetone and ethanol prior to use. Zinc nitrate hexahydrate, hexamethylene tetramine, toluene, potassium permanganate, hydrazine hydrate, sodium hydroxide, zinc acetate dihydrate, and isopropylidene malonate were purchased from Alfa Aesar and used as received. Perchloric acid (50%) and nitric acid (70%) were used as received from Fisher Scientific. Epon 862 and Epikure 9553 were received from Momentive Inc. and used as received.

Fiber Functionalization Reactions. The fibers are functionalized through five separate surface treatments. A hydrazine reduction treatment removes some of the oxygen functional groups. Hydrazine reduced fibers were created by placing IM-8 fibers into a 10% solution of ultrapure water and hydrazine hydrate. The fibers were refluxed for eight hours, then washed thrice in ultrapure water and dried at 100 °C for several hours. A defect grafting technique selectively converts existing defect sites to carboxylic acid groups. Defect grafted fibers were synthesized by refluxing IM-8 fibers in a 0.05 M solution isopropylidene malonate in toluene for 2 h.[38] The fibers were then washed with Soxhlet extraction for 8 h in ultrapure water and then dried at 100 °C for several hours. Selective oxidation reactions preferentially oxidize existing functional groups without creating new functional groups. Selective oxidation of fibers began by using an ultrasonic cleaner to dissolve 90 mg of potassium permanganate in 21 mL of perchloric acid and 20 mL of water. The mixture was then

poured over 6 cm of IM-8 fibers, and after 10 min the solution was quenched with 42 mL of 0.0148 M citric acid. The fibers were then washed in ultrapure water three times and dried at 100 °C. Oxidative techniques were used to substantially increase the oxygen functional groups without any preference to the specific chemistry of the groups. Nitric acid oxidation began by refluxing 6 cm of IM-8 carbon fibers in 100 mL of 70% nitric acid for 4 h. After oxidation, the fibers were cleaned with water through Soxhlet extraction for 8 h. The fibers were then cleaned in ultrapure water in an ultrasonic cleaner eight times for 3 min and then dried at 100 °C. Some of these fibers were then subjected to the same reduction procedure listed earlier to create the reduced − acid oxidized fibers.

X-ray Photoelectron Spectroscopy. Fibers to be analyzed by XPS were vacuum dried at 100 °C for 4 h and then loaded into a high vacuum exchange chamber ($<2 \times 10^{-8}$ mbar) overnight prior to sample analysis. All experiments were performed with a pressure of less than 1.5×10^{-9} mbar. Carbon fibers with 3 cm lengths were mounted underneath copper masks with stainless steel screws to avoid contamination from hydrocarbon sources like double-sided tape. All data were collected on a VG ESCALAB 220i-XL and processed using CASA-XPS. All samples were excited by an Al k-α (1486 eV) monochromated x-ray source, and a through-the-lens electron flood gun was used to compensate any charge losses. Electrons were collected at a 90° take-off angle and X-rays excited the fibers from an angle of 45° from the axis of the fiber. Corrections of less than 2 eV were applied to some of the samples in order to align the main C1s peak at 284.7 eV. Each high resolution spectrum was first fit with a Shirley background and then decomposed into four components, one for each oxidation state, to fit the data. Fitting was performed with the aid of CASAXPS using the built in Marquette regression function, with the initial fit starting from the authors' best attempt. Each data set was fit with curves (a Gaussian 70% − Lorentzian 30% mixture, GL30) that were constrained in location and FWHM to realistically model the chemistry of the fiber and capability of the instrumentation, respectively. The instrumentation was calibrated for peak width on a sample of commercially available highly oriented pyrolytic graphite (NT-MDT, Zelenograd, Moscow, Russia), which resulted in a peak width of 0.6 eV. All peaks had a constrained FWHM of 1.1−1.7 eV, and peaks were constrained at 284.5−285.5 eV, 285.5−287.0 eV, 286.5−288.0 eV, and 288.0−290.0 eV. It was observed through a series of preliminary samples that occasionally the low binding energy side of the peak would not match the GL30 curve shape because the fiber to mask contact was not always sufficient. The residuals of all data at binding energies higher than the main C−C peak were tested for normality with a χ^2 test, assuming an estimated mean and variance, and a 5% confidence level.[38]

Growth of the ZnO Nanowire Interphase. The ZnO nanowire growth began with the synthesis of a suspension of ZnO nanoparticles following the methods developed by Hu et al.[39] Briefly, a 0.02 M solution of sodium hydroxide in ethanol and a 0.0125 M solution of zinc acetate dihydrate in ethanol were made by heating and then cooling ethanol to 65 °C under vigorous stirring. 24 mL of the NaOH solution was then added into 60 mL of absolute ethanol and preheated to 65 °C. 24 mL of the zinc acetate solution was added to 192 mL of ethanol and also preheated to 65 °C. The two solutions were then mixed with vigorous stirring and heated at 65 °C for 45 min in a sealed glass jar to yield 300 mL of seeding suspension. The suspension was then allowed to cool to room temperature. Single carbon fibers were mounted to nylon frames with Devcon 5 minute epoxy and then cleaned sequentially in boiling acetone and boiling ethanol. After cleaning, any uncured epoxy was leached off the frame by placing the frame into boiling water for 10 min. After cleaning, the fibers mounted on the frames were dipped in the seed suspension and annealed in a convection oven for 10 min at 150 °C. After 10 min, the frame was allowed to cool for 5 min before dipping into the seed suspension, annealing for 10 min and cooling for 5 min. After seeding the fibers three times, the frame was allowed to cool and then placed into a preheated solution of 0.001 M hexamethylenetetramine and 0.001 M $Zn(NO_3)_2 \cdot 6H_2O$ in water. The fibers remained in the 90 °C growth solution for 150 min at which point the beaker was flooded with

ultrapure water to wash away the growth solution and remove floating ZnO particles inside the growth solution. This procedure was the same regardless of the surface treatment applied to the fiber.

Mechanical Testing of Fibers and Composites. The tensile strength was measured by testing 20 fibers with a Favimat+ fiber testing machine (Monchengladbach, Germany) with a 25.4, 12.7, or 6.35 mm gauge length. Weibull distributions were fit to both the ultimate stress and strain distributions for each set of fibers, including 95% confidence intervals on the parameter estimates. In lieu of capturing and measuring each fiber diameter, 35 of the original fibers were measured and the average (5.45 μm) assumed to be constant for all subsequent tensile measurements. Epon 862 and Epikure 9553 were mixed 100:16.9 pbw in a small cup. Single fiber composites were created by placing the ZnO nanowire coated carbon fibers into silicone rubber molds and filling with the polymer. The strong, tough epoxy polymer did not necessitate pretension of the fibers as the matrix itself can undergo upwards of 10% strain before failure, which was found to be sufficient to saturate the length of the fiber with cracks. The polymer was gelled at 40 °C for 1 h, then demolded and placed in a convection oven at 100 °C for 1 h, followed by 160 °C for 1 h. The samples were then polished and tested in a custom microtensile frame under the microscope. A combination of transmitted polarized light and reflected light enabled clear observance of cracks that developed to prevent erroneous measurements.

Molecular Dynamics Simulations. MD simulations were performed using large-scale atomic/molecular massively parallel simulator LAMMPS[40] to calculate the adhesive energy of individual function groups on the surface of the carbon fiber. The surface of the carbon fiber was modeled with single layer of graphite (graphene) with functional groups attached on the surface. Graphene and the functional groups were modeled with the optimized potentials for liquid simulations OPLS-AA.[41] The parameters are shown in Tables 1

Table 1. State Concentrations of Surface As Measured by XPS

peak location (eV)	C−C carbon (284.7) (%)	C−O hydroxyl (286.5) (%)	C=O ketone (287.5) (%)	COOH carboxyl (289.0)
reduced IM8	78.6	15.0	3.6	3.0
IM8	68.0	17.3	9.5	5.2
defect grafted	66.1	7.3	13.5	13.1
selectively oxidized	73.3	10.0	8.0	8.7
reduced − acid oxidized	62.1	20.3	12.2	5.3
acid oxidized	52.0	22.0	16.6	9.3

and 2. ZnO was modeled using the Buckingham potential,[42] the unknown parameters were obtained from mixing rules, and the Ewald method[43] was used to take in account of the charges. The ZnO slab was periodic in X and Y directions, leaving the (0001) and (000$\bar{1}$) free polar surfaces because ZnO NWs grow along the (0001); thus the polar surface of ZnO is parallel to the surface of the carbon fiber. The polar surfaces of ZnO are Tasker type III,[44] and in this structure the accumulation of electrostatic energy causes the energy to diverge at the surface leading to instability of the structure; here the structure was stabilized by removing 1/4 of the zinc atoms on the (0001) surface.[44] The graphene edges were terminated by hydrogen atoms to stabilize the structure. Initially the structure was relaxed using the isothermal−isobaric ensemble (NPT),[45] and zero stress was obtained in all directions for both ZnO and graphite.

■ RESULTS AND DISCUSSION

Fiber Functionalization. Carbon fibers were functionalized to produce a variety of chemical states on the surface of the fiber. This study focuses on the chemistry at the interface; thus it is imperative that surface sensitive techniques be

Table 2. Bonded Interaction for the Model of ZnO−Graphene with Functional Groups, C=O, COH, COOH[a]

bond	length (Å)	K/2 (kcal/mol)	bend	angle (deg)	K/2 (kcal/mol)
C−C (G)	1.40	234.5	C−C−C	120	31.5
C−H (G)	1.08	183.5	C−C−H	120	17.5
C−C^a (G)	1.51	158.5	C−C−C^a	120	35.0
C^a−C (K)	1.522	158.4			
C=O (K)	1.229	285.0			
C−O (H)	1.410	160.0	C−O−H	108.5	27.5
O−H (H)	0.945	276.5			
C=O (C)	1.229	285.0	O=C−O	121	40.0
C−O (C)	1.364	225.0	C−O−H	113	17.5
O−H (C)	0.945	276.5			
torsion	K	D	n		
	3.625	180	2		
improper	K	Xo			
	1.10	0.0			

[a]C^a is the anchor carbon on the basal plane; ( ) denotes G-graphene, K-ketone, H-hydroxyl, C-carboxylic acid.

employed to determine the molecular structure of the fiber surface, not the bulk. X-ray photoelectron spectroscopy (XPS) is a surface-sensitive technique with a sampling depth of approximately 1 nm and is used here to identify the functional groups on the surface of the fibers. Furthermore, XPS peak intensity scales linearly, and thus the technique can effectively provide quantitative measurements of the concentration of each functional group on the surface. Unfortunately, XPS does not have great chemical specificity because the instrument measures core electrons that are not direct participants in the covalent bonds. Nevertheless, XPS provides a useful characterization of the surface by indicating the polarity of the bonds, which can measure the chemical environment at the surface.

Alternative characterization methods, in particular, Fourier transform infrared spectroscopy, can resolve highly specific chemical structures. Unfortunately, FTIR spectroscopy is not widely used in the characterization of carbon fiber surfaces because the black body absorption of graphite overwhelms any signals that may arise. More than this, FITR is a poor tool in the study of carbon fiber surfaces because it is not surface sensitive. Even with surface measuring techniques, such as attenuated total reflectance, the relatively high refractive index of graphite means that sampling depths can easily exceed 500 nm, meaning the effective concentration of the surface functional groups desired is less than 0.1%, below standard thresholds for FTIR. In spite of these problems, we attempted at various points to try to confirm XPS measurements with various forms of FTIR measurements, both transmitted and reflectance methods, and on each occasion we were unable to collect meaningful data. Analyzing the surfaces of carbon fibers could be performed with Auger electron spectroscopy (AES), or secondary ion mass spectroscopy (SIMS) as well. AES does not have the chemical specificity required to delineate between the alternative species since they would often have the same elements (carbon, oxygen) and SIMS would most likely prove too complex to definitively analyze because the fragments would include several overlapping windows of atomic mass. A survey of the literature shows that XPS and AFM remain the preferred methods for surface analysis.[46]

Carbon fiber is primarily graphitic and consists of carbon and oxygen, with most of the oxygen concentrated at the surface of the fiber. For the polyacrylonitrile-based IM8 fibers used in this work, there is occasionally a small concentration of nitrogen from the precursor that does not diffuse out of the fiber during production. Nitrogen concentrations tend to be less than 1% and exist throughout the fiber with no preference to exist at the surface and thus do not form an important part of the chemical environment at the surface. Previous XPS survey scan data from other researchers is consistent with our finding that no significant peaks, other than carbon and oxygen, are present on the fiber surface.[47] The atomic composition implies that the carbon on the surface of the fiber is primarily in carbon−oxygen or carbon−carbon bonds, which will help guide the analysis by narrowing down the possible structures. Carbon fibers exist with functional groups at the surface; however these groups can be arranged in a nearly infinite number of molecular configurations with differing chemical behavior. The limitations of XPS prevent the discernment of the specific molecular structure of the surface; however the polarity of the bonds of the carbon can be resolved. Thus, the fibers used in this work will be characterized by the relative fraction of carbon atoms in four different bonding states: 0 carbon −oxygen bonds, 1 carbon−oxygen bonds, 2 carbon−oxygen bonds, and 3 carbon−oxygen bonds. Although these peaks contain a variety of specific chemical groups, the peaks will be named the carbon peak, the hydroxyl peak, the ketone peak, and carboxyl peak. While not entirely consistent with the chemical definitions, some form of nomenclature is required for the purposes of this article.

The fitting of each of the four peaks is somewhat challenging with XPS data and must be justified. The relative separation of the four peaks is 1−1.5 eV, with all four peaks located somewhere between 284.5 eV and 289.5 eV. Many XPS instruments are calibrated from the C1s peak; however this could be convoluted with the signal and thus serves as a poor calibration for these experiments. Gold is known to covalently bond with very few substances; thus the Au4f peaks are highly repeatable and serve as an excellent indicator of the impact of each aspect of the instrument. Although the sampling resolution of the instrument can be as little as 0.1 eV, experiments to calibrate the peak width of Au4f show a minimum practical peak width of about 0.65 eV.[48,49]

Resolving peak separation of 1.0 eV requires information about the fiber a priori and the use of a fitting algorithm to create repeatability in the measurements. For this work, an understanding that only oxygen and carbon will be significantly present on the surface helps narrow down the number of peaks to be fit. Then, constraints are applied to the four peaks and the Marquardt regression algorithm is allowed to converge on the solution to provide the concentration of each functional group on the surface of the fiber. The constraints applied to the fitting create conditions where the fitting algorithm can give additional meaning and interpretation to the data collected. The four peaks were constrained first with limits on location, with the ranges being 284.5−285.5, 285.5−287.0, 286.5−288.0, 288.0−289.5. Each peak is constrained to have a peak width of 1.1−1.7 eV. The lower resolution limit corresponds to a best-case estimate of practical instrument resolution, while the upper limit was determined based upon initial manual fitting. All curves were fit according to these parameters to remove as much human intervention as possible from the data analysis. While the peak locations indicate the number of carbon−oxygen bonds, the specific location of each peak varies with each data set. The fitting algorithm, instrument variation, and

most significantly the exact chemical structure can lead to variations in the fitted peak location of nearly 0.5 eV, necessitating the windows on each state location. As stated earlier, different molecules or molecular structures will vary the binding energy of a C1s core electron; however these variations fall below the peak width of most measurements, and thus while they influence the data trends of this precision become impossible to distinguish. In summary, while the peak locations will vary slightly between measurements, peak intensity in the general bands outlined above can be positively correlated with the number of carbon−oxygen bonds.

Infinite control over the degree oxidation is not permitted with most functionalization treatments. Thus, for this work, control is provided by creation of multiple functionalization treatments, each one enabling a different chemical environment on the surface of the fiber. The techniques include traditional oxidation, chemical reduction, selective oxidation, and a novel non-oxidative method. These five methods not only create more or less total oxygen groups, but they also modulate the relative proportions of each functional group. Varying and controlling the surface chemistry enables this work to determine the dominant functional groups in the adhesion of a ZnO nanowire interphase on carbon fibers. The following paragraphs will introduce each functionalization method and mechanism, and then compare the techniques relative to one another. Certainly, the functionalization procedures attempted in this work are by no means a replicate of all of the published fiber functionalization methods. Alternatives exist and were considered; however several of those methods overlap in the functional groups created. Lastly, the impact of each functionalization on the fiber tensile strength is discussed.

The removal of oxygen functional groups from carbon fiber is difficult through thermal methods because the intense thermal treatments during fiber manufacture make it unlikely that more thermal reduction will be effective and irreversible. Hydrazine hydrate has been shown to be extremely effective in the reduction of graphene oxide, and this process was adopted to remove some oxygen functional groups from the surface of the fiber. High resolution C1s XPS data show the fiber has fewer oxygen functional groups than the fiber as received. Hydrazine is effective for reducing the carboxyl groups to ketones and hydroxyls and for removing epoxide and hydroxyl groups entirely. The reaction mechanism for a hydrazine reduction is shown in Figure 1A. The hydrazine reduction mechanism does

not include the removal of C−C bonds and can even serve to restore them in some instances. Hydrazine is not a strong acid capable of intercalating the fiber either, and etching of the fiber or the opening of subsurface pores is not expected during the reduction. These factors should prevent the reduction technique from reducing the fiber tensile strength. Figure 2 shows that the tensile strength of the reduced fiber is not significantly different from the IM8 fiber as received.
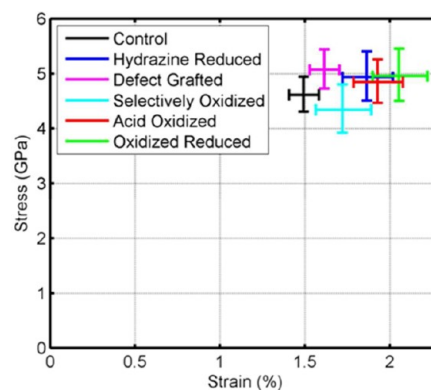

Figure 2. Tensile strength of each of the functionalized fibers. Each set of errorbars represents the 95% confidence intervals on the scale parameter of a Weibull distribution fit the ultimate stress and strain sets of data.

The second technique employed is selective oxidation through potassium permanganate. Permanganate ions in acid solutions are highly oxidative; however they are most reactive at high temperatures. The selective oxidation procedure used here was performed at room temperature, which creates a substantial difference in the energy required to oxidize an existing functional group compared to oxidizing a C−C bond. As such, the selective oxidation preferentially oxidizes existing functional groups to ketones and carboxyl groups, without significantly damaging the tensile properties of the fiber. The selective oxidation mechanism is shown in Figure 1B; specifically the figure shows the oxidation of a hydroxyl group to a ketone. This method was borrowed from another graphite allotrope, the carbon nanotube.[50,51] Selective oxidation, or upconversion, is often employed on carbon nanotubes after an acid oxidation to convert arbitrary oxygen functional groups into carboxylic acid groups. At low temperatures, it does not induce unzipping of the tubes or destruction of the C−C bonds. The structural carbon fibers in this experiment do not suffer damage or etching by the reaction; simply the reaction conditions are too mild to damage the fiber. Figure 2 confirms that selective oxidation does not damage the fiber tensile strength.

The third technique employed is a defect grafting technique with isopropylidene malonate, or Meldrum's acid. Meldrum's acid is a heterocycle, susceptible to nucleophilic attack which induces a ring-opening reaction, as shown in Figure 1C. Naturally occurring hydroxyl groups can initiate this, while many other functional groups do not. After the ring-opening, a malonic ester grafts onto the fiber. This short molecule is terminated in a carboxylic acid group, effectively replacing a hydroxyl surface group with a carboxylic acid group. This technique provides control over the relative concentration of functional groups, creating more carboxylic acid and fewer hydroxyls. The grafting of a short molecule creates multiple
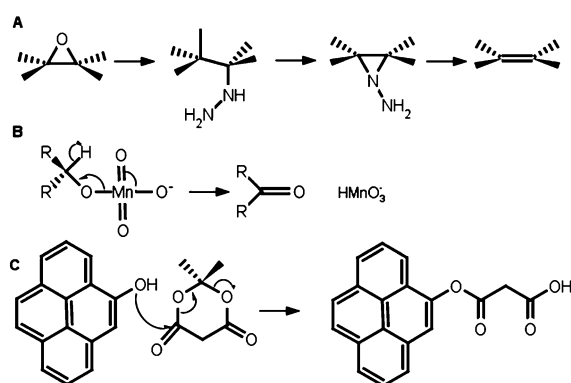
Figure 1. Functionalization reactions used in this work to adjust the fiber surface chemistry. (A) Hydrazine reduction reaction mechanism to remove oxygen groups. (B) Selective oxidation method. (C) Defect grafting method to attach carboxyl terminated esters.
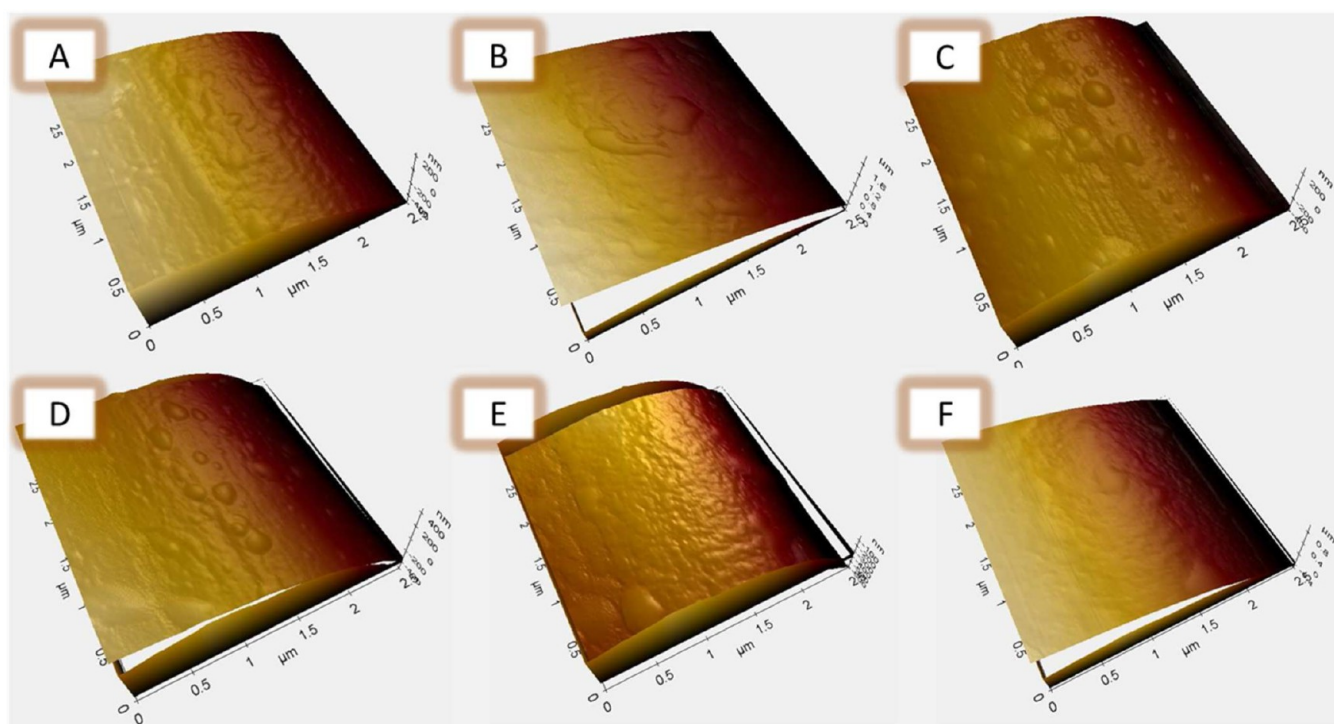
Figure 3. Fiber surface profiles measured with AFM. None of the fibers show a significant change in the surface profile. The fibers are (A) hydrazine reduced, (B) IM8, (C) selectively oxidized, (D) defect grafted, (E) reduced acid oxidized fibers, and (F) nitric acid oxidized fibers.

new carbon states that must be accounted for in the analysis of the XPS data. The grafting of a short molecule to existing defects will not decrease the strength of the fiber or etch the surface, so long as the reaction solvent is not destructive to graphite. Previous research has proven that the defect grafting technique does not reduce the tensile strength of the fibers, nor does it etch or pit the surface.[38] The previous report of this defect grafting study confirms that regardless of reaction conditions employed, the fiber tensile strength is maintained.

The remaining two techniques are based on a traditional oxidative method, specifically nitric acid oxidation from the work by Gardner et al.[26] Nitric acid oxidation has the capability to etch and oxidize the fibers, creating many hydroxyl and ketone groups. The process can damage the fiber, and thus any oxidative functionalization must be accompanied by tensile data. For this work, the specific IM8 fiber and nitric acid oxidation procedure used appears to not damage the fiber itself, as indicated in Figure 2. It should be noted that we have also attempted this functionalization with T600 and AS4 carbon fibers and found the fibers to be unrecognizable after treatment; thus these results are not necessarily extensible to alternative PAN-based carbon fibers. The last two methods created are related, first one fiber as oxidized and one fiber oxidized and then reduced with hydrazine. The nitric acid oxidation creates large numbers of oxygen functional groups, some of which are removed by the reduction procedure, to adjust the surface chemistry. Nitric acid oxidation does not show a preference for which functional groups it oxidizes, neither theoretically from the reaction mechanism, nor experimentally from surface observations. The oxidation procedures developed for these two fibers were tuned to minimize damage to the fiber surface, adjusting the time of oxidation. Figure 2 clearly shows that the tensile strength of the fibers is not reduced after oxidation or reduction.

Each fiber surface after functionalization was examined for etching or pitting that might indicate that the reaction was too aggressive. Etching has two profound effects on the conclusions to be drawn later. First, etching defects into the fibers is the primary method in which the tensile strength of the fibers is reduced. Small fibers derive many of their extraordinary properties from the reduced probability of defects in the fiber, but the creation of additional defects act as stress concentrations and initiate failure in the fiber. Second, the assumptions of this work rely upon the fiber–interphase bonding to have the same surface area and surface roughness in each case, as this is well known to influence interfacial bonding. Atomic force microscopy (AFM) images of each of the six fibers are shown in Figure 3, and it is clear that the surface of the fibers is not significantly changed by any of the functionalization procedures.

The tensile strength of the fibers is unaffected in three of the five reactions because of the specific reaction mechanism employed. For the hydrazine reduction reaction, few defects are created because the hydrazine is not capable of intercalating or breaking apart the graphitic bonds. The hydrainze simply removes carbon–oxygen bonds and the associated functional groups, thus maintaining the surface and number of defects. The selective oxidation reaction does not affect tensile strength because it preferentially reacts with existing functional groups and does not oxidize the carbon–carbon double bonds characteristic to graphitic structures. The selective oxidation, although it contains perchloric acid, occurs quickly at low temperatures and in the absence of sulfuric acid. This differs from traditional graphite oxide reactions where the combination of perchlorates and strong acids can intercalate graphite. The defect grafting reaction employs mild solvents (toluene) and relatively low temperatures (110 °C) that do not affect carbon fibers. The remaining two reactions include a nitric acid

functionalization reaction, whereby a strong acid is used to oxidize the fiber. Echoing the comments earlier, we have observed that IM8 fibers are resistant enough to the oxidation to minimize reductions in the tensile strength, in contrast with alternatives such as AS4 or T600 fibers.

The XPS data have been compiled in Figure 4. The area of each peak as fit by the regression algorithm is included in Table
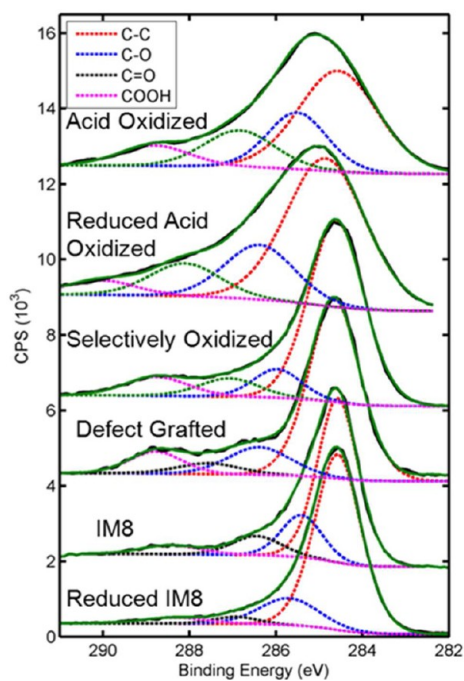
Figure 4. Compiled XPS data showing the variety of functional group combinations created with the functionalization procedures above. The table shows the relative concentration of each functional group fitted to the data.

1. The curves in Figure 4 show increasing area of the oxygen functional group peaks. Furthermore, although it is difficult to assess through the curves, the fits listed in the table show that each functionalization procedure produces different relative intensities of each functional group. Some procedures, by the nature of the chemical reaction, preferentially create specific functional groups, and thus a variety of chemical environments can be achieved. Figures 2, 3, and 4 all indicate that the functionalization procedures change the surface chemistry of the fiber and create different combinations of oxygen functional groups, without affecting the tensile strength or the surface roughness of the fibers.

ZnO Nanowire Growth. Previous work on the development of the ZnO nanowire interphase has shown that the interfacial shear strength depends, in part, on the morphology of the nanowires on the fibers.[20] Longer, larger nanowires increase the interfacial shear strength because they have a larger gradient to distribute the load across, and the larger diameter reduces the amount of polymer in contact with the nanowire surface. The nanowires used in this work were approximately 750 nm long and 70 nm in diameter and are shown on typical fibers in Figure 5. The deposition of ZnO nanowires on the fiber surface begins with a seed layer of ZnO nanoparticles that nucleate into ZnO nanowires. The ZnO gradually precipitates out of the aqueous growth solution, preferentially depositing on the nanoparticles rather than nucleating in free solution. The

Table 3. Nonbonded Interactions for the Model ZnO-Graphene with Functional Groups C=O, COH, COOH[a]

	atom	σ (Å)	ε (kcal/mol)	q (e)
graphene	C	3.4	0.0556	0.0
	C^a	3.4	0.0556	0.08
COOH	C	3.75	0.1049	0.55
	=O	2.96	0.2099	−0.50
	O	3.0	0.1700	−0.58
	H	0.0	0.0000	0.45
COH	C	3.4	0.0556	0.08
	O	3.07	0.1700	-0.70
	H	0.00	0.0000	0.435
C=O	C^a	3.4	0.0556	0.08
	C	3.75	0.1050	0.47
	=O	2.96	0.2100	-0.47
Buckingham parameters				
pair	A	C	r	
Zn−Zn	220190.498	738.007	0.21916	
O−O	0.0	0.0	1×10^{-10}	
Zn−O	12216.328	0.0	0.3581	

[a]The charges for Zn atom is +2 and O -2 in ZnO slab. C^a is the anchor carbon on the basal plane.
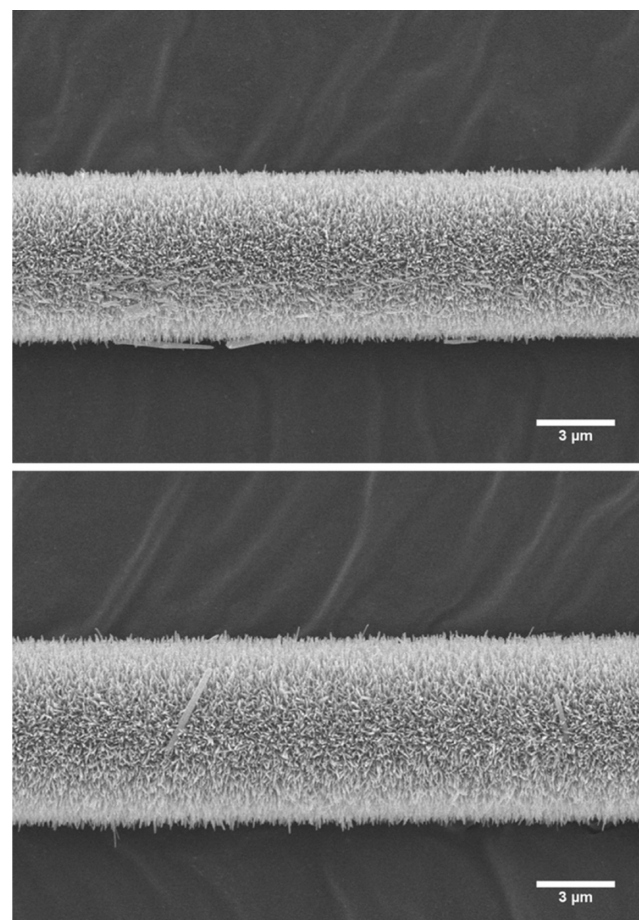
Figure 5. Typical ZnO nanowires grown on carbon fiber for use in this work. The nanowires are approximately 750 nm long and 70 nm in diameter. The two pictures are of separate fibers, indicating that the process is very repeatable.

nanowires grow as single crystals and deposit as nanowires because the [0001] polar face has approximately 10 times the

growth rate of the lateral faces. The crystallite size of the nanowires is equivalent to the observed size in Figure 5 because the nanowires are single crystalline in nature. The nanowires in this experiment maintain the aspect ratio of approximately 10, consistent with previous works.[37] The architecture employed in this study was previously conceived and characterized by Lin et al.[17] and is very similar to that published by Ehlert et al.[18] These reports demonstrate that the nanowires have a wurtzite structure and begin growth from a polycrystalline seed layer.

The growth of the nanowires is largely unaffected by the surface chemistry at the surface of the fiber. Although the fibers each have a different surface, the growth begins with the deposition of a polycrystalline ZnO seed layer. The seed layer is a complete shell that forms around the surface of the fiber, effectively blocking the surface of the fiber from the growth solution. As such, we conclude the material within the boundaries of the fiber is entirely carbon fiber. The material just beyond the surface of the fiber is entirely polycrystalline ZnO seeds. The nanocomposites interphase is a mixture of ZnO nanowires with the 0001 plane oriented outward from the fiber surface, and the volume fraction gradually reduces with increasing radial position. Finally, beyond the nanowires, the material is entirely polymer matrix. The creation of the seed layer is formed by dipping the fibers into a colloidal suspension of ZnO nanoparticles, which deposit onto the fiber. The nanoparticles are then annealed into a polycrystalline film to nucleate the subsequent nanowires. The nanowires grown on the surface of the fibers is consistent from fiber to fiber, so long as the seeds were synthesized according to the same procedure. Previous works have shown that the growth of ZnO nanowires on the surface of the fibers has no impact on the tensile strength of the fibers because the deposition occurs at such low temperatures in a benign aqueous solution.[17,33,52] In other words, a ZnO coated fiber has the same tensile strength as the fiber prior to growth.

Interfacial Shear Strength. The ZnO−fiber interface must be the interface of failure if the effect of fiber functionalization is to be observed. Previous results[17−19] show that failure during pullout occurs at the ZnO−fiber interface. This was expected as the fiber−ZnO interface has the lowest surface area and no interlocking that would make it stronger than the ZnO−polymer interface. This work builds upon those previous results and begins with the assumption that the fiber−ZnO interface is the interface of failure. The interfacial shear strength was measured through single fiber fragmentation testing.[53] Single fiber fragmentation testing enables a high degree of quality control as a single fiber can be grown on and then tested without excessive handling and great certainty over the nanowire consistency. Single fiber fragmentation measures the interfacial shear strength by subjecting a dilute single fiber composite to tensile strain. The strain applied begins to fracture the fiber into smaller and smaller fragments, until the surface area of each fragment is insufficient to fracture the fiber again. With knowledge of the tensile strength, the interfacial shear strength can be estimated by measuring the fiber surface area of the average fiber length. A photograph of the test setup and a micrograph of a series of fiber cracks are shown in Figure 6.

The interface strength of each fiber was measured using single fiber fragmentation testing. The interface strength was then compared to the concentration of each functional group present on the surface of the fiber, using the previous XPS data listed in Figure 4. The interface strength, shown in Figure 7, was then analyzed for correlation to the concentration of each
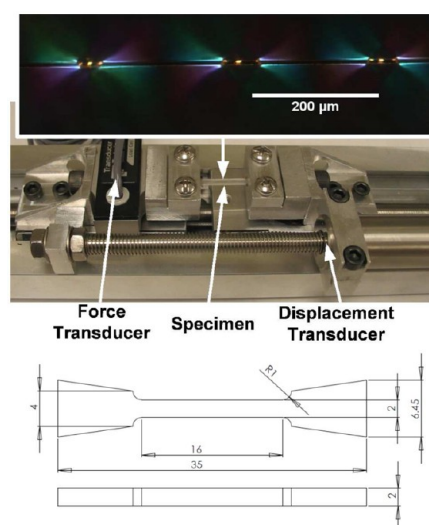

Figure 6. Single fiber fragmentation test experimental setup showing the specimen, grips, and transducers. The micrograph above it shows typical cracks in the fiber under a combination of polarized and transmitted light to highlight the cracks. Below are the dimensions (mm) of the specimens tested.

functional group. Four plots are shown in Figure 7. Four linear fits were computed: specifically interface strength as a function of hydroxyl groups, ketone groups, carboxyl groups, and as a sum of the three groups (total oxygen functional groups). The coefficient of determination (R^2) value for each fit was computed to be 0.89, 0.47, 0.87, 0.13, respectively, which are displayed on the corresponding plots. R^2 is defined as $R^2 = 1 - \Sigma_i(y_i - f_i)^2/\Sigma_i(y_i - \overline{y}_i)^2$ where y_i is the observed data point and f_i is the fitted data. R^2 is a common statistical measure of how well a regression curve fits the data, or more precisely the reduction in error attributed to the regressed curve. It is clear that the correlation between interface strength and the total concentration of oxygen groups (sum of hydroxyl, ketone, carboxyl groups) is strong. In analyzing the contribution of each functional group, it is clear that carboxyl or hydroxyl group concentrations do not correlate with the interfacial shear strength. The concentration of ketone functional groups clearly has a strong correlation with interface strength. Ketone groups have two readily accessible lone pairs of electrons that are naturally oriented outward from the surface. Hydroxyl groups have a pH-dependent proton attached to them, which can interfere with the ability of the functional group to interact with the ZnO nanoparticle.

This report of experimental evidence that ketone groups provide the adhesion for ZnO nanowires in carbon fiber composites has far reaching implications. The selective creation of ketone groups through chemical procedures such as the Corey−Kim oxidation, Swern oxidation, or various grafting techniques could significantly improve the adhesion without significant cost to the mechanical properties of the fibers. Improvements to the chemical adhesion of ZnO nanowires to carbon fiber composites also stands to improve the overall effectiveness of ZnO nanowires for improving interface strength because the weakest interface remains the fiber−nanowire interface.

It is well known that interfacial shear strength impacts, both negatively and positively, the tensile strength of a lamina scale composite. The tensile failure of a composite often involves several phenomena, notably crack propagation through and/or
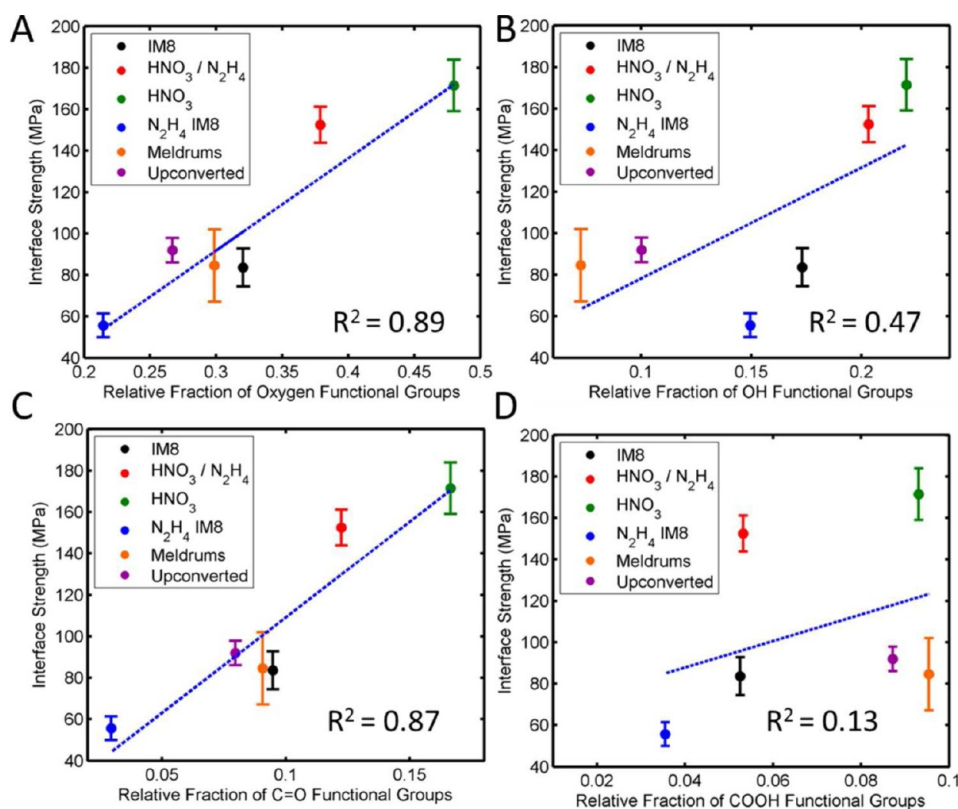
Figure 7. Interfacial shear strength of six different fibers with ZnO nanowires grown on the surface. Each subplot shows the correlation of interfacial shear strength with a specific functional group, as measured from the high resolution C1s data with XPS. The figures show correlation with (A) total oxygen functional groups, (B) hydroxyl groups ($\sim$285.5 eV), (C) ketone groups ($\sim$287.0 eV), and (D) carboxylic acid groups ($\sim$289.5 eV). The legend in each figure lists IM8 fibers as received, acid oxidized then hydrazine reduced IM8 fibers, acid oxidized IM8 fibers, hydrazine reduced IM8 fibers, defect grafted IM8 fibers, and selectively oxidized IM8 fibers.

along the interface of the fibers. This study focuses on identifying the adhesion of a ZnO nanowire interphase to carbon fibers suitable for structural composites, and thus lamina scale measurements are not included. For this study, we use single fiber fragmentation testing, which infers interface strength from the known tensile strength of the fiber. Many other researchers, particularly those focusing on hybrid fibers with a carbon nanotube interphase, have shown that single fiber fragmentation is suitable for estimating interface strength of fibers with differing tensile strengths. In this work, the measured tensile strength of each fiber is used in the computation of interface strength, and thus we follow the methods developed previously in the study of interfaces.[54,55]

Molecular Dynamics Simulation. The molecular dynamics simulations were used to predict the energy required to separate a ZnO slab from a graphene sheet, with and without oxygen functional groups present on the face of the graphene sheet. Initially NPT ensemble as implemented in LAMMPS was used to obtain zero stress at the X and Y boundaries of ZnO. Specifically, the temperature was set to 100 K and the system was simulated for 20 ps with the temperature gradually reduced to 1 K in the interval of 20 ps while keeping the NPT ensemble. Graphene was terminated by hydrogen atom at the edge with the purpose to have a structrure with zero stress independent of LAMMPS's simulation box. Once the system was at the minimum energy and with zero residual stress on both ZnO and graphene the NVT esemble was used to allow control of the temperature and apply constraints to simulate liftoff. The separation was performed by fixing the upper

surface of the ZnO slab and the graphene was separated at steps of 0.25 Å with the structure equilibrating for 20 ps before the next step to obtain a velocity of 1.25 m/s. The force was recorded at each time step, and the adhesive energy was calculated from the resulting force–displacement curve. The first simulation separated pristine graphene from the ZnO and the atomic models are shown in Figure 8A. The energy to separate ZnO from pristine graphene was 2.734 aJ and normalizing by the area of graphene surface 896 Å^2 yields a specific adhesive energy of 0.303 J/m^2. Three types of functional groups, each corresponding to the primitive functional group categories measured with XPS, were added with surface concentrations of 1.6%, 3.3%, and 5%. The same procedure was followed to calculate the adhesive energy for each functional group and coverage fraction. Figure 8B shows the interfacial energy computed for each of the MD simulations. The interfacial energy is insensitive to the relative coverage of the hydroxyl functional groups and carboxylic acid functional groups. Both hydroxyl and carboxylic acid functional groups include hydrogen atoms, which can interfere with the ability of the ZnO to interact with the surface. Ketone groups contrast with hydroxyl and carboxyl groups in that they do not have any hydrogen atoms to interfere with bonding and have two accessible lone pairs that can strongly interact with the Zn atoms in the ZnO crystal. The high polarity of the ketone groups strongly interacts with the Zn ions in the crystal, while the lone pairs in hydroxyl or carboxyl groups are either partially shielded by the proton or sterically hindered by the molecule. Figure 8B shows that the interfacial energy increases with the
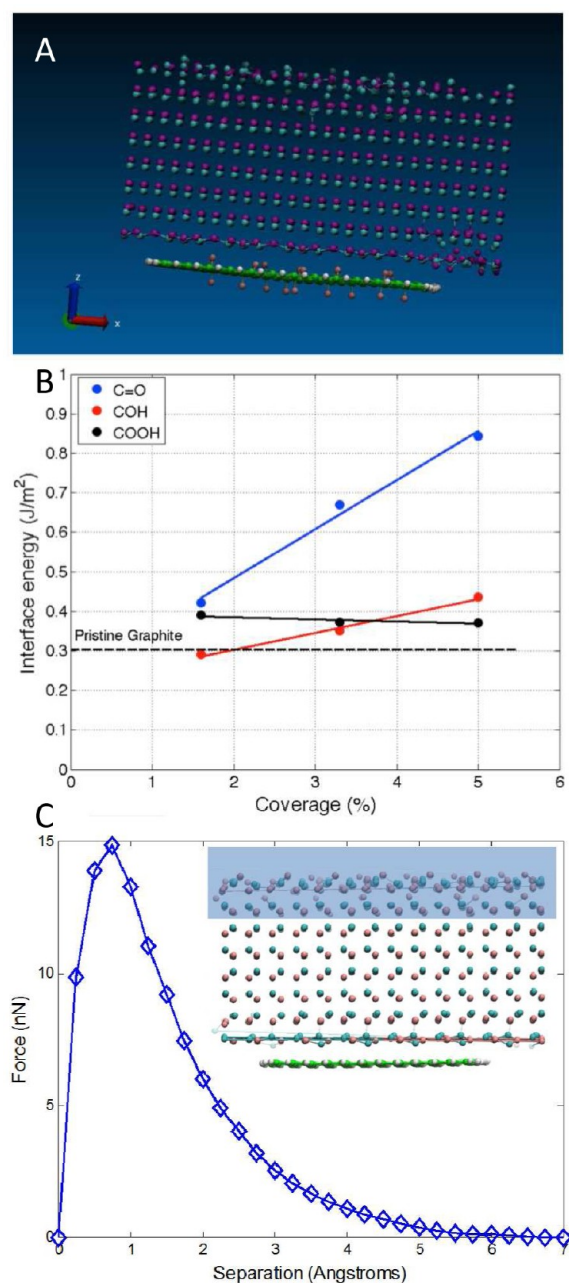
Figure 8. Simulation results computing the energy to separate a ZnO crystal from a functionalized graphene sheet. (A) Model showing relaxed structure of the functionalized graphene sheet and ZnO crystal. (B) Interface energy required to separate the ZnO crystal from the functionalized graphene sheet. (C) Force displacement curve generated at each relaxation step during the separation.

fraction of functional groups and that the addition of ketone functional groups can increase interfacial energy beyond what is achievable with pristine graphite or the other classes of functional groups. This trend is consistent with the experimental observations that showed increases in the interfacial shear strength correlate with increasing ketone functional groups measured by XPS. The creation of additional ketone groups through selective reactions is expected to be the most efficient method for increasing the adhesion of ZnO nanowires. Evidence in both the experiments as well as the simulations shows the preference of ZnO with ketone groups in controlling adhesion.

CONCLUSION

The chemical mechanism of adhesion between a ZnO nanowire interphase and a carbon fiber has been investigated. Five different chemical functionalization procedures were applied to carbon fiber and the tensile strength of the fibers after treatment was measured in all cases. The chemistry of the surface was analyzed with XPS to assess the functional groups present on the surface. The interfacial shear strength of six different fiber surfaces was shown to correlate with not only the quantity, but also preferentially with specific types of functional groups present on the surface. Correlation between interface strength and ketone groups was the highest, owing to the limited steric hindrance of the two lone pairs on the oxygen atom. Experimental evidence was confirmed with MD simulations of the separation of ZnO from a graphene surface. The computational results confirm that ketones are most prominent in adhesion because the lone pairs are accessible and not blocked by protons attached elsewhere on the molecule. The identification of the most prominent groups in adhesion can help improve other ZnO nanowire reinforced composites by directing future research; specifically for ZnO, methods should be sought for the selective creation of ketone groups on carbon fiber. This presentation of a method for the identification of the chemical mechanism of adhesion can extend to alternative whiskerization materials, demonstrating how these materials might be developed in the future.

AUTHOR INFORMATION

Corresponding Author
*E-mail: Gregory.ehlert.ctr@wpafb.af.mil. Present Address: Non-metallic Materials Division, Materials and Manufacturing Directorate, Air Force Research Laboratory, 2941 Hobson Way, Wright-Patterson AFB, OH 45433.

Notes
The authors declare no competing financial interest.

ACKNOWLEDGMENTS

ABBREVIATIONS

CFRPs = continuous fiber reinforced polymers
CNTs = carbon nanotubes
XPS = X-ray photoelectron spectroscopy
AFM = atomic force microscope

REFERENCES

(1) Gibson, R. F. *Principles of Composite Material Mechanics*; CRC Press: Boca Raton, 2007.
(2) Milewski, J. V.; Shyne, J. J. US003580731, 1967.
(3) Rand, B.; Robinson, R. *Carbon* **1977**, *15*, 257−263.
(4) Waltersson, K. *Composites Sci. Technol.* **1985**, *22*, 223−239.
(5) Proctor, A.; Sherwood, P. M. A. *Carbon* **1983**, *21*, 53−59.
(6) Proctor, A.; Sherwood, P. M. A. *Surf. Interface Anal.* **1982**, *4*, 212−219.
(7) Zielke, U.; Hüttinger, K. J.; Hoffman, W. P. *Carbon* **1996**, *34*, 999−1005.
(8) Delamar, M.; Désarmot, G.; Fagebaume, O.; Hitmi, R.; Pinsonc, J.; Savéant, J. M. *Carbon* **1997**, *35*, 801−807.

(9) Zhdan, P. A.; Grey, D.; Castle, J. E. *Surf. Interface Anal.* **1994**, *22*, 290−295.

(10) Zhdan, P. A.; Bors, M.; Castle, J. E. *Composites Sci. Technol.* **1998**, *58*, 559−570.

(11) *Handbook of Fiberglass and Advanced Plastics Composites*; R. E. Krieger Publishing Co.: Huntington, NY, 1975.

(12) Milewski, J. V.; Shyne, J. J.; Shaver, R. C. Whiskers and Their Composites; Lubin, G., Ed.; In *Handbook of Fiberglass and Advanced Plastic Composites*; Krieger Publishing Co.: Huntington, NY, 1969; Vol. 1, pp 255−281.

(13) Qian, H.; Greenhalgh, E. S.; Shaffer, M. S. P.; Bismarck, A. *J. Mater. Chem.* **2010**, *20*, 4751−4762.

(14) Sager, R. J.; Klein, P. J.; Lagoudas, D. C.; Zhang, Q.; Liu, J.; Dai, L.; Baur, J. W. *Compos. Sci. Technol.* **2009**, *69*, 898−904.

(15) Zhang, Q.; Liu, J.; Sager, R.; Dai, L.; Baur, J. *Compos. Sci. Technol.* **2009**, *69*, 594−601.

(16) Kowbel, W.; Bruce, C.; Withers, J. C.; Ransone, P. O. *Composites Part A: Applied Science and Manufacturing* **1997**, *28*, 993−1000.

(17) Lin, Y.; Ehlert, G.; Sodano, H. A. *Adv. Funct. Mater.* **2009**, *19*, 2654−2660.

(18) Ehlert, G. J.; Sodano, H. A. *ACS Appl. Mater. Interfaces* **2009**, *1*, 1827−1833.

(19) Ehlert, G. J.; Lin, Y.; Galan, U.; Sodano, H. A. *J. Solid Mech. Mater. Eng.* **2010**, *4*, 1687−1698.

(20) Galan, U.; Lin, Y.; Ehlert, G. J.; Sodano, H. A. *Compos. Sci. Technol.* **2011**, *71*, 946−954.

(21) Krekel, G.; Zielke, U. J.; Hüttinger, K. J.; Hoffman, W. P. *J. Mater. Sci.* **1994**, *29*, 3984−3992.

(22) Zielke, U.; Hüttinger, K. J.; Hoffman, W. P. *Carbon* **1996**, *34*, 1015−1026.

(23) Waltersson, K. *Compos. Sci. Technol.* **1985**, *23*, 303−321.

(24) Pittman, C. U., Jr; Jiang, W.; He, G. -.; Gardner, S. D. *Carbon* **1998**, *36*, 25−37.

(25) Pittman, C. U., Jr; He, G. -.; Wu, B.; Gardner, S. D. *Carbon* **1997**, *35*, 317−331.

(26) Gardner, S. D.; Singamsetty, C. S. K.; Wu, Z.; Pittman, C. U., Jr. *Surf. Interface Anal.* **1996**, *24*, 311−320.

(27) Wang, Y.; Zhang, F.; Sherwood, P. M. A. *Chem. Mater.* **1999**, *11*, 2573−2583.

(28) Wang, Y.; Zhang, F.; Sherwood, P. M. A. *Chem. Mater.* **2001**, *13*, 832−841.

(29) Viswanathan, H.; Wang, Y.; Audi, A. A.; Allen, P. J.; Sherwood, P. M. A. *Chem. Mater.* **2001**, *13*, 1647−1655.

(30) Zhdan, P. A.; Bors, M.; Castle, J. E. *Compos. Sci. Technol.* **1998**, *58*, 559−570.

(31) Drzal, L. The Interphase in Epoxy Composites; Dušek, K., Ed.; In *Epoxy Resins and Composites II*; Springer: Berlin/Heidelberg, 1986; Vol. 75, pp 1−32.

(32) Downs, W. B.; Baker, R. T. K. *Carbon* **1991**, *29*, 1173−1179.

(33) Galan, U.; Lin, Y.; Ehlert, G. J.; Sodano, H. A. *Compos. Sci. Technol.* **2011**, *71*, 946−954.

(34) Qian, H.; Bismarck, A.; Greenhalgh, E. S.; Shaffer, M. S. P. *Carbon* **2010**, *48*, 277−286.

(35) Zhong Lin, W. *Mater. Sci. Eng., R: Rep.* **2009**, *64*, 33−71.

(36) Greene, L. E.; Law, M.; Tan, D. H.; Montano, M.; Goldberger, J.; Somorjai, G.; Yang, P. *Nano Lett.* **2005**, *5*, 1231−1236.

(37) Greene, L. E.; Yuhas, B. D.; Law, M.; Zitoun, D.; Yang, P. *Inorg. Chem.* **2006**, *45*, 7535−7543.

(38) Ehlert, G. J.; Lin, Y.; Sodano, H. A. *Carbon* **2011**, in review.

(39) Hu, Z.; Oskam, G.; Searson, P. C. *J. Colloid Interface Sci.* **2003**, *263*, 454−460.

(40) S., P. *J. Comput. Phys.* **1995**, *117*, 1−19.

(41) Jorgensen, W. L.; Maxwell, D. S.; Tirado-Rives, J. *J. Am. Chem. Soc.* **1996**, *118*, 11225−11236.

(42) Binks, D. J. *Computational Modelling of Zinc Oxide and Related Oxide Ceramics*; University of Surrey; Guildford, Surrey, United Kingdom, 1994.

(43) Darden, T.; York, D.; Pedersen, L. *J. Chem. Phys.* **1993**, *98*, 10089−10092.

(44) Tasker, P. W. *J. Phys. C: Solid State Phys.* **1979**, *12*, 4977.

(45) Andersen, H. C. *J. Chem. Phys.* **1980**, *72*, 2384−2393.

(46) Ehlert, G. J. *Development of a Zinc Oxide Nanowire Interphase for Enhanced Structural Composites*; University of Florida: Gainesville, Florida, USA, 2012.

(47) He, X.; Zhang, F.; Wang, R.; Liu, W. *Carbon* **2007**, *45*, 2559−2563.

(48) Briggs, D.; Briggs, D. *Handbook of X-ray and Ultraviolet Photoelectron Spectroscopy*; Heyden: London, 1977.

(49) Beamson, G.; Briggs, D. *High Resolution XPS of Organic Polymers: the Scienta ESCA300 Database*; Wiley: New York, 1992.

(50) Kordás, K.; Mustonen, T.; Tóth, G.; Jantunen, H.; Lajunen, M.; Soldano, C.; Talapatra, S.; Kar, S.; Vajtai, R.; Ajayan, P. *Small* **2006**, *2*, 1021−1025.

(51) Jeong, W.; Kessler, M. R. *Chem. Mater.* **2008**, *20*, 7060−7068.

(52) Ehlert, G. J.; Sodano, H. A. *ACS Appl. Mater. Interfaces* **2009**, *1*, 1827−1833.

(53) Feih, S.; Wonsyld, K.; Minzari, D.; Westermann, P.; Lilholt, H. **2004**, *Risø-R-1483*.

(54) Sager, R. J.; Klein, P. J.; Lagoudas, D. C.; Zhang, Q.; Liu, J.; Dai, L.; Baur, J. W. *Compos. Sci. Technol.* **2009**, *69*, 898−904.

(55) Thostenson, E. T.; Li, W. Z.; Wang, D. Z.; Ren, Z. F.; Chou, T. W. *J. Appl. Phys.* **2002**, *91*, 6034.